

Received 4 November 2023, accepted 27 December 2023, date of publication 5 January 2024,
date of current version 18 January 2024.

Digital Object Identifier 10.1109/ACCESS.2024.3350141

RESEARCH ARTICLE

Relationship for Electric Network Between Internal Voltage Amplitude/Frequency Stimulation and Active/Reactive Power Response and Its Characteristics Analysis

RONGXIN SUN¹, (Student Member, IEEE), WEI HE¹, (Member, IEEE),
AND XIAOMING YUAN, (Senior Member, IEEE)

State Key Laboratory of Advanced Electromagnetic Engineering and Technology, School of Electrical and Electronic Engineering, Huazhong University of Science and Technology, Wuhan 430074, China

Corresponding author: Wei He (hewei5590@hust.edu.cn)

This work was supported in part by the National Key Research and Development Program of China under Grant 2022YFB2402701.

ABSTRACT The process, in which the internal voltage with time-varying amplitude and frequency (A/F) regulated by equipment generates the electric network's terminal power variations, plays a critical role in the system dynamic. For the system dynamic analysis, the relationship between the time-varying A/F and the power response, as well as its characteristics, is required. However, this subject has yet to be emphasized and thoroughly studied due to insufficient attention to the fact that the frequency is time-varying. In traditional power system analysis, since the network's time constant is often fast enough compared to synchronous generators, the electric network is generally depicted by the static relationship with the assumption of constant frequency, although it is not consistent with the practice of frequency time-varying. Moreover, in the present renewable generation scenario, the fast A/F dynamics of internal voltages can impact the power response, and further the system dynamics. So that adequate investigations around the electric network's power response in relation to the time-varying A/F are more urgent. Motivated by these considerations, this paper studies the network's original relationship between the internal voltage's A/F stimulation and the active/reactive power response, which contains the oscillatory integral problem in math. By using the method of integration by parts, an explicit expression of this relationship is given. Further, a simplified relationship is presented to help understand the dynamic characteristics of the network. Several unusual observations, including the composition and consumption on the line of the active/reactive power in relation to the time-varying A/F, are obtained.

INDEX TERMS Electric network, internal voltage, time-varying amplitude/frequency, active/reactive power.

I. INTRODUCTION

Dynamic process analysis is the basis for ensuring the safe and stable operation of power systems [1], [2]. In dynamic processes of power systems, such as post-fault transients, oscillations, frequency dynamics, etc., the amplitude and frequency (A/F) of the power equipment's internal voltage and the voltages throughout the grid are observed to vary

The associate editor coordinating the review of this manuscript and approving it for publication was Guangya Yang¹.

with time [3], [4], [5], [6], [7]. For example, the different dynamics of the voltage amplitude and frequency observed in the 2006 European grid accident [4], as shown in Fig. 1, and the 2020 Australian grid oscillation phenomenon [6], as shown in Fig. 2. Such time-varying A/F voltages generate what variations in the electric network's terminal power determine the dynamic behaviors of power equipment, and naturally play a critical role in the system dynamic [1], [8]. Thus, to analyze the system dynamic and reveal the stability mechanism, it is required to know the power generation in

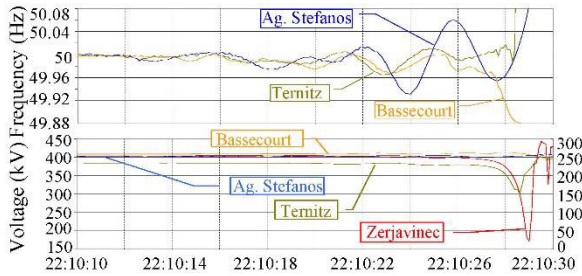


FIGURE 1. The measured waveform of the voltage frequency/amplitude in the disturbance event of the continental European transmission grid on November 4, 2006.

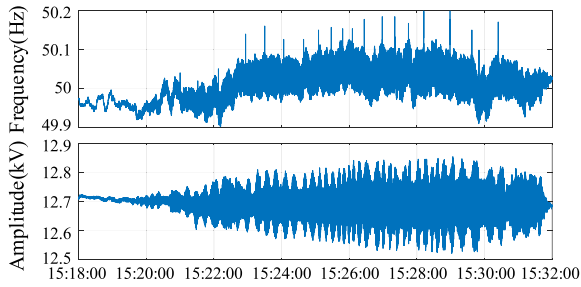


FIGURE 2. The measured waveform of the voltage frequency/amplitude in oscillations event of the West Murray area on May 25, 2020.

relation to the time-varying A/F voltage. Moreover, with the rapid increase of renewable energy and other power electronic-based equipment in power systems, the variations characteristics of AC voltage's A/F are more complex, as shown in Fig. 2, making this problem more salient in today's power system [7], [8].

While the A/F variation over time is observed in practice, there is a lack of full understanding of the original physical meaning of the time-varying instantaneous frequency, which is the basis for obtaining the relationship between the power and the time-varying A/F voltage. In general, the frequency is described as the number of times an AC waveform repeats itself per second [9], [10], [11]. However, this is not appropriate in system dynamics [12], [13], [14]. In power systems, the instantaneous frequency actually represents the rotation vector's angular velocity, i.e., the instantaneous angular frequency [15]. This is because power systems rely on the equipment's internal voltage to generate the necessary voltage for the electric network, and the internal voltage is determined by adjusting the angular velocity and length of the voltage's rotating vector [2], [15]. For example, synchronous machines generate their internal voltage by the excitation winding rotation, where the rotor speed and the excitation current determine the instantaneous angular frequency and length of the internal voltage's rotating vector [15], [16]. Similarly, the converter-interfaced equipment also forms the instantaneous angular frequency and length of the internal voltage's rotating vector by its multi-timescale controls, and then by modulation transformations to generate the expected three-phase AC voltage through a hardware or software oscillator [17], [18], [19], [20], [21]. Without loss of generality, the word "frequency" in this paper refers

to angular frequency. When the system is disturbed, the equipment is subjected to terminal power changes. As a result, unbalanced active/reactive power adjusts the A/F of the internal voltage, which in turn changes the current along the line and the network's terminal active/reactive power to restore the balance [8]. Therefore, the voltage's frequency at each position, as well as the amplitude, exhibits instantaneous variations over time during system dynamics.

Since the equipment adjusts the instantaneous A/F of the internal voltage acting on the electric network to change terminal power, the relationship establishment of the power response to the time-varying A/F stimulation is required to serve for understanding and analyzing the system dynamic. However, the basic question of how to depict the original relationship of the time-varying A/F resulting in the corresponding changes in network power has not been directly considered in system dynamic analysis. In fact, the basic mathematical form of this original relationship, given the electric network inductive properties, contains the oscillatory integral problem that has received extensive attention in mathematics for a long time [22], [23], [24], [25].

In the traditional power system analysis, the static network relationship with the "quasi-steady state" assumption of constant frequency is generally used in many studies and calculations, such as the small perturbation analysis, transient stability analysis, etc. [26], [27], [28], [29], [30]. However, this assumption fails to fully reflect the fact that the frequency is time-varying during system dynamics. In fact, the static network relationship can be traced back to Fortescue, who pointed out that it was a static condition in analyzing system power limitations in the 1920s [31]. Some research found that the frequencies are unequal at different positions during system dynamics, often attributed to electromechanical waves [32], [33], [34], [35]. Nevertheless, even those in-depth studies in this area are still based on the static network relationship and do not study the network's original relationship when the frequency changes over time. Furthermore, some studies recognized the limitations of the static network relationship and pointed out that the analysis results of traditional power system transient stability and small perturbation stability may not be consistent with practice in some scenarios [36], [37], [38], [39]. Moreover, in the present renewable generation scenarios, the fast A/F dynamics of internal voltages can impact the current and further the system dynamics, so that the static network relationship is not further suitable in such scenarios [40], [41], [42]. Various Fourier-based methodologies of periodic harmonics, such as the dynamic phasor method, attempted to overcome the limitation of the static network relationship [43], [44], [45]. However, these methods tell only the waveform compositions without tracing back to the physical origin of the time-varying A/F and its relation to the active/reactive power response, thus offering limited insights into understanding the mechanics of system dynamics. It can be seen that the current research can not sufficiently meet the needs of system analysis, especially in renewable energy generation scenarios.

With the above considerations and based on the physical meaning of instantaneous frequency, this paper expects to provide a foundation and aims to illustrate the method of establishing the electric network relationship between the time-varying A/F and the active/reactive power. This study presents the explicit expressions of this network relationship for the oscillatory integration problem it contains based on the generalized mathematical method of integration by parts, using the inductive network as an illustration. Interestingly, a time-varying A/F voltage, when applied to an inductive component, will produce not only an orthogonal but also an in-phase current component, which is unforeseen from common understanding and is expected to stimulate a renewed consideration of the network's impacts on system dynamics. In addition, this paper also presents a network's simplified relationship for the relatively slow changing rate of A/F to help understand the network characteristics in dynamics. On this basis, it presents several observations, especially the physical mechanism of the terminal active/reactive power generation in relation to the internal voltage's time-varying A/F and its potential impact on the system dynamics, as well as active/reactive power consumption on the inductive line for understanding power (energy) balancing in system dynamics.

The rest of this paper is organized as follows. Section II illustrates the internal voltage formation mechanism and the system's closed-loop regulation process. The inherent nature of internal voltage's time-varying A/F in power system dynamics and the necessity of the network relationship between the time-varying A/F and the active/reactive power response are presented. Section III elaborates on the method of establishing the network stimulation-response relationships and gives the original explicit expressions of a network as an example. Section IV presents a simplified relationship to help build an intuitive understanding of the physical mechanism of the terminal power generation in relation to the internal voltage's time-varying A/F, including its potential impact on the system dynamics. Section V presents the network power response under various equipment's time-varying A/F, and its properties are verified based on simulations. Finally, several conclusions are drawn, and some related issues are discussed in Section VI.

II. THE CLOSED-LOOP REGULATION MECHANISM OF SYSTEMS AND THE NECESSITY OF NETWORK'S STIMULATION-RESPONSE RELATIONSHIP

A. CLOSED-LOOP REGULATION PROCESS OF POWER SYSTEM

Power system's operation relies on the electric equipment's internal voltage to establish the AC voltage of the electric network. The equipment forms the three-phase AC waveforms of its internal voltage by determining the length (i.e., instantaneous amplitude) and angular velocity (i.e., instantaneous frequency) of the internal voltage vector [15]. According to the literatures [15] and [17], Fig. 3 shows the details of how the synchronous generator and converter-based

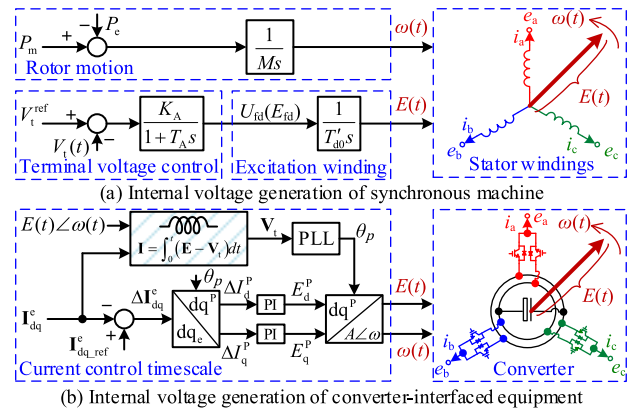


FIGURE 3. Generation of the internal voltage rotating vector.

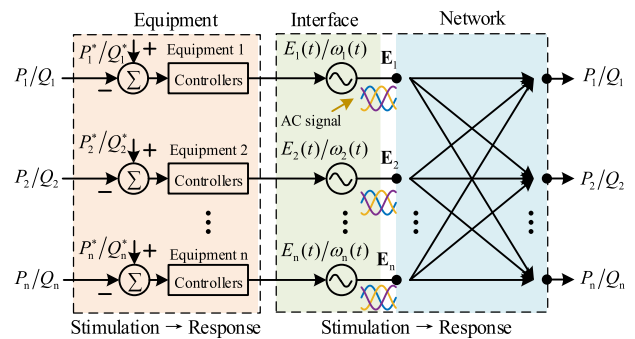


FIGURE 4. Schematic diagram of the system's closed-loop relationship.

equipment generate their internal voltages to facilitate further illustration.

When the power system is subjected to disturbances, the terminal active/reactive power of the power equipment changes. The equipment's output power is unbalanced with its input. Then, the controllers (e.g., governor, excitation system, alternating current control, etc.) respond to regulate the internal voltage's A/F [17]. The variations in A/F result in changes in the AC wave of the internal voltage, which acts on the network to change the AC current. Thus, the active/reactive current variations and the active/reactive power exchanged between the network and the equipment change. This process lasts until the input-output power of the equipment is restored to balance. Thus, the system dynamic presents the closed-loop dynamic regulation between the A/F of the equipment's internal voltage and the network's terminal active/reactive power [8], as depicted in Fig. 4.

It is clear that the A/F of the equipment's internal voltage exhibits time-varying characteristics in the system dynamic. Hence, the expressions of the rotating vector and three-phase instantaneous value should be presented as in (1).

$$\begin{cases} \mathbf{E} = E(t)e^{j\theta(t)} = E(t)e^{j\left(\int_0^t \omega(\tau)d\tau + \varphi_0\right)} & \text{rotating vector} \\ e_a = E(t) \cos\left(\int_0^t \omega(\tau)d\tau + \varphi_0\right) & \text{wave depicted by A/F} \end{cases} \quad (1)$$

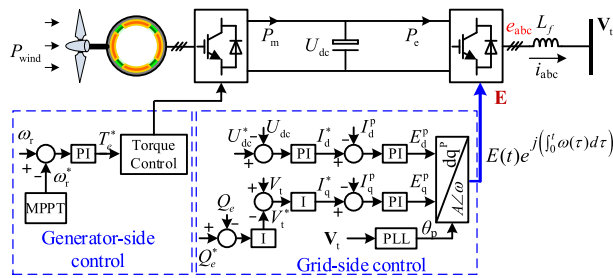


FIGURE 5. The control structure of the GE type-4 wind turbine.

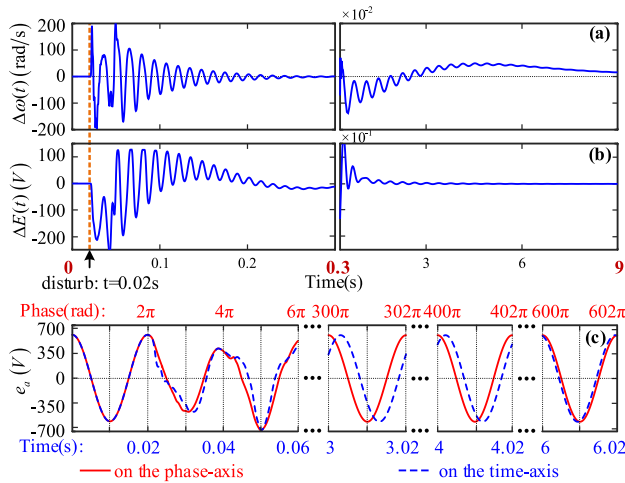


FIGURE 6. Response of the time-varying A/F and the instantaneous values of the internal voltage at phase-A.

where φ_0 is the initial phase, $E(t)$ and $\omega(t)$ are the time-varying instantaneous amplitude and frequency, respectively. The e_a is the internal voltage of phase-A.

A simulation case is presented to show further the process of the equipment regulating its instantaneous A/F to change the AC waveform of the internal voltage in the system dynamic. A type-4 wind turbine is used as an example, and the control structure is shown in Fig. 5. The simulation is based on the 3-machine 9-bus system, occurring short circuit fault on line 7-8 lasted 0.02 s, as shown in Appendix. As seen in Fig. 6 (a) and (b), the A/F of the wind turbine’s internal voltage regulated by its controllers exhibits variations with fast and slow dynamics on different timescales. While the instantaneous frequency varies with time, the internal voltage’s AC waveform changes on the phase-axis and on the time-axis are different, as shown in Fig. 6 (c) after 0.02s. The different dynamic characteristics of A/F will lead to different features in AC waveforms. Combining Fig. 6 and (1), it can be observed that when the A/F exhibits fast timescale dynamics (as shown in 0.02–0.3s), the fast and slow alternating changes in a cycle make the AC waveform appear like harmonics inside. When the A/F exhibits slow timescale dynamics (as shown in 0.3–3s), the waveform on the time-axis within multiple alternating waveforms with high (or low) frequency shortens (or lengthens) the alternating time interval, and over time, the alternating time of the waveform will change noticeably due to the effect of the instantaneous frequency

deviating from the rated frequency. It is clear that the AC waveforms are not periodic in the system dynamic, as shown in Fig. 6 (c), and cannot be described by the harmonics with a fundamental frequency.

B. NECESSITY OF THE NETWORK’S RELATIONSHIP BETWEEN THE TIME-VARYING A/F AND ACTIVE/ REACTIVE POWER FOR SYSTEM ANALYSIS

Based on the above system’s closed-loop regulation process, it can be seen that the equipment regulates the instantaneous A/F of the internal voltage acting on the network. Thus, the power variations in the network are always the result of the instantaneous A/F change of these internal voltages. When analyzing the system dynamics, it is always inevitable to pay attention to the power generated from the instantaneous A/F of the internal voltage. An explicit expression of the network relationship between the time-varying A/F and active/reactive power is needed, but it is currently lacking.

Consequently, according to the requirements of system dynamic stability analysis, this paper establishes the explicit expression of the network relationship between the time-varying A/F and the active/reactive power. Besides, with this relationship to build the system model, the basic structure (equipment and network) and their functions are naturally separated, which leads to structured modeling of the power system. Therefore, the equipment’s dynamic characteristics can be depicted uniformly through the relationships between the imbalance of input/output power stimulation and the internal voltage’s A/F response, described by the equipment’s motion equation. Much work has been done in this area [15], [16], [17], [18], [19], [20], [21]. Correspondingly, the network dynamic characteristics are depicted by the relationships between the internal voltage’s A/F stimulation and active/reactive power response. The following section will elaborate on the concept and method of establishing the network relationships.

III. MODELING METHOD OF THE NETWORK BASED ON STIMULATION-RESPONSE RELATIONSHIPS

This section begins with a single line as an example to facilitate illustration. It illustrates the challenges and concepts of establishing network relationships through detailed derivation of the line’s two-terminal stimulation–response relationships. It also elaborates on the challenge of obtaining explicit expressions from the well-known relationships of AC instantaneous values. Then, this process is combined to elaborate on the generalized establishment method of the network’s relationship based on the time-varying A/F stimulation of multiple internal voltages and the terminal power response.

A. ESTABLISHING THE RELATIONSHIP OF A SINGLE LINE

We take the two-machine system shown in Fig.7 as an example. The network includes the equipment’s internal inductance, transformers inductance, and lines inductance. The total equivalent inductance is $L = L_{g1} + L_{T1} + L_{line} +$

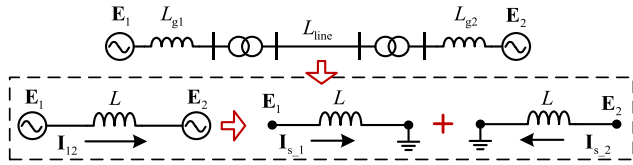


FIGURE 7. Decomposition of the current throughout the line.

$L_{T2} + L_{g2}$. According to the law of electromagnetic induction, the line instantaneous current can be separately decomposed into the current components excited by each internal voltage,

$$\begin{aligned} \mathbf{I}_{s_1} &= \frac{1}{L} \int_0^t E_1(\tau) e^{j\theta_1(\tau)} d\tau, \\ \mathbf{I}_{s_2} &= -\frac{1}{L} \int_0^t E_2(\tau) e^{j\theta_2(\tau)} d\tau \end{aligned} \quad (2)$$

where $\mathbf{I}_{12} = \mathbf{I}_{s_1} + \mathbf{I}_{s_2}$. Equation (2) also can be expressed with other forms in $\alpha\beta$ and other coordinates [17]. The current vector is projected on the voltage vector to obtain the active/reactive current and the active/reactive power. Thus, Fig.8 shows the complex nonlinear relationships between the A/F and the power, including the exponential operation (Part 1), integral operation (Part 2), orthogonal decomposition (Part 3), and multiplication (Part 4). Although the active/reactive power is essentially a function of the internal voltage's time-varying A/F, their direct relationships are not explicitly stated, concealing in the four-part operations. The following presents the process to obtain the explicit expressions of the network relationships.

First, the current needs to be directly expressed in terms of the internal voltage's A/F instead of AC instantaneous values. However, the (2) is typically the "oscillatory integral problem" in mathematics, and it cannot be expressed using finite-term elementary functions [22], [23], [24], [25]. This problem is irrelevant to the coordinate choice. This paper uses the asymptotic method, which employs integration by parts to expand the oscillatory integral into the series form. Taking terminal 1 as an example:

$$\begin{aligned} \mathbf{I}_{s_1} &= \frac{1}{L} \int_0^t E_1(\tau) e^{j[\int_0^\tau \omega_1(s) ds + \varphi_{10}]} d\tau \\ &= \frac{E_1(\tau)}{j\omega_1(\tau)L} e^{j\theta_1(\tau)} \Big|_0^t - \int_0^t \left(\frac{E_1(\tau)}{j\omega_1(\tau)L} \right)' e^{j[\int_0^\tau \omega_1(s) ds + \varphi_{10}]} d\tau \\ &= \frac{E_1(\tau)}{j\omega_1(\tau)L} e^{j\theta_1(\tau)} \Big|_0^t - \frac{1}{j\omega_1(\tau)} \left(\frac{E_1(\tau)}{j\omega_1(\tau)L} \right)' e^{j\theta_1(\tau)} \Big|_0^t + \dots \\ &= \left(\sum_{b=1}^{\infty} (-j)^b A_{1_b} \right) e^{j\theta_1(\tau)} \Big|_0^t = \left(I_{s_1}^d(t) + jI_{s_1}^q(t) \right) e^{j\theta_1(t)} \end{aligned} \quad (3)$$

where superscript " ' " indicates the derivative with time. The expressions for each term are as follows:

$$A_{1_1} = \frac{E_1(t)}{\omega_1(t)}, \quad A_{1_2} = -\frac{1}{\omega_1(t)} A'_{1_1}, \dots,$$

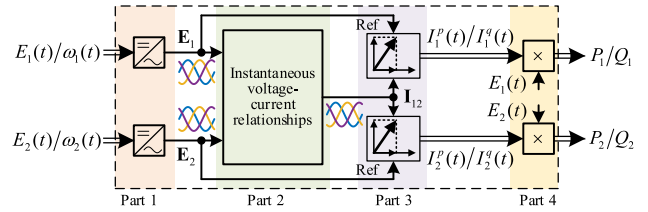


FIGURE 8. The nonlinear relationship between the A/F and the power.

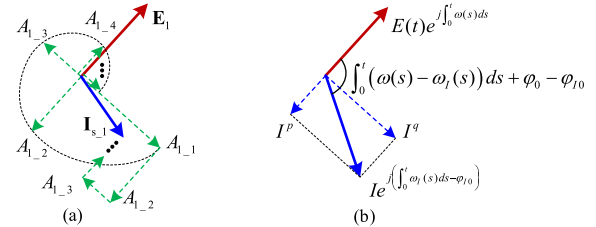


FIGURE 9. Geometric diagram of (a) the series expansion based on the asymptotic method, (b) decomposition of the active/reactive current.

$$A_{1_b} = -\frac{1}{\omega_1(t)} A'_{1_b-1}, \dots$$

The current is decomposed into components differed by 90° in sequence, as shown in Fig. 9 (a). As shown in (3), it is worth mentioning that a time-varying A/F voltage, when applied to an inductive component, will produce not only an orthogonal component $I_{s_1}^q(t)$ but also an in-phase current component $I_{s_1}^d(t)$. The orthogonal and in-phase components respectively generate the active and reactive power, which is unforeseen from common understanding. Fig. 10 depicts this physical phenomenon. In the case of constant A/F, the AC voltage (same situation as Fig. 6) generates only an orthogonal current over an inductive component. In the system dynamic, the phase of the AC current and the phase of the AC voltage no longer differ by 90 degrees, as shown in Fig. 10 (a). It indicates that the AC voltage generates both the in-phase (green line) and orthogonal (red line) current components, as shown in Fig. 10 (b).

Secondly, each current component is split orthogonally into active and reactive currents with the internal voltage. As shown in Fig. 9 (b), the current vector's components are projected on the voltage vector to obtain the in-phase and orthogonal components $I_{1x}^P(t)/I_{1x}^Q(t)$, which correspond to the active and reactive current components, respectively. The active/reactive current multiplies with the internal voltage's amplitude, and the active/reactive power is obtained. The operation is as follows.

$$\begin{aligned} \frac{3}{2} \mathbf{E}_1 \cdot \bar{\mathbf{I}}_{s_x} &= \frac{3}{2} E_1(t) \left(I_{s_x}^d(t) \cos \delta_{1x}(t) + I_{s_x}^q(t) \sin \delta_{1x}(t) \right) \\ &\quad + j \frac{3}{2} E_1(t) \left(I_{s_x}^d(t) \sin \delta_{1x}(t) - I_{s_x}^q(t) \cos \delta_{1x}(t) \right) \\ &= \frac{3}{2} E_1(t) \cdot I_{1x}^P(t) + j \frac{3}{2} E_1(t) \cdot I_{1x}^Q(t) \end{aligned} \quad (4)$$

where $x=1$ or 2 , and $\delta_{1x}(t) = \int_0^t (\omega_1(\tau) - \omega_x(\tau)) d\tau + \varphi_{10} - \varphi_{x0}$.

Then, the active/reactive power is obtained from (2) and (4).

$$S_1 = \frac{3}{2} \mathbf{E}_1 \cdot \bar{\mathbf{I}}_{s_1} + \frac{3}{2} \mathbf{E}_1 \cdot \bar{\mathbf{I}}_{s_2} = P_{s_11} + jQ_{s_11} + P_{m_12} + jQ_{m_12} \quad (5)$$

The power at terminal 1 consists of four components, where P_{s_11}/Q_{s_11} is the power components generated by \mathbf{E}_1 separately, and P_{m_12}/Q_{m_12} is the power components generated by \mathbf{E}_1 and \mathbf{E}_2 together. To provide a clear illustration, the power component independently stimulated by each internal voltage is termed the power's self-component, and its corresponding current component is termed the current's self-component. The power component jointly stimulated by different internal voltages is termed the power's mutual component, and its corresponding current component is termed the current's mutual component.

Finally, by combining (3) and (5), the power's self/mutual components can be expressed with the time-varying A/F of each internal voltage, which is as follows:

$$P_{s_11} = \frac{3E_1(t)}{2} \sum_{b=1}^{\infty} (-1)^b A_{1_2b} \quad ,$$

$$Q_{s_11} = \frac{3E_1(t)}{2} \sum_{b=1}^{\infty} (-1)^{b+1} A_{1_2b-1}$$

$$P_{m_12} = \frac{3E_1(t)}{2} \sum_{b=1}^{\infty} (-1)^b (A_{2_2b} \cos \delta_{12}(t) + A_{2_2b-1} \sin \delta_{12}(t))$$

$$Q_{m_12} = \frac{3E_1(t)}{2} \sum_{b=1}^{\infty} (-1)^{b-1} (A_{2_2b-1} \cos \delta_{12}(t) - A_{2_2b} \sin \delta_{12}(t))$$

It shows that the internal voltage generated terminal power that contains components separately dependent on the A/F of itself and the others. Thus, each terminal's power has self and mutual components with different physical meanings concerning time-varying A/F of different internal voltages.

B. GENERALIZED ESTABLISHING METHOD FOR NETWORK'S MULTIPLE TERMINAL STIMULATION-RESPONSE RELATIONSHIPS

1) METHOD AND PROCESS OF ESTABLISHING THE NETWORK'S RELATIONSHIP

The above derivation can be extended to a general method for establishing the network's multiple terminal stimulation-response relationships. First, it is necessary to express the line current as an explicit analytical expression in terms of the internal voltage's time-varying A/F. Next, the time-varying A/F current components are orthogonally decomposed on the reference of the given terminal's internal voltage to obtain the self/mutual components of the active/reactive current and the self/mutual components of the network's terminal active/reactive power. Finally,

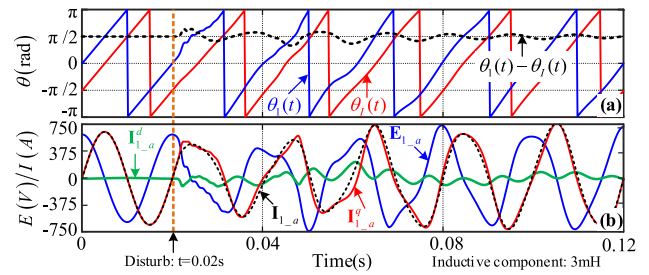


FIGURE 10. The time-varying A/F voltage generates the in-phase and orthogonal current components.

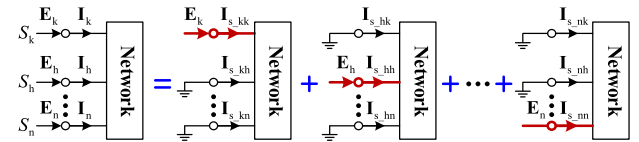


FIGURE 11. Decomposition of the current into components of voltage acting alone.

each power's self/mutual component is added to obtain the output active/reactive power at the given terminal. Detailed instructions are provided below.

Step 1. Decompose the current into components generated by each internal voltage individually.

To help systematically derive the relationships of all internal voltages' time-varying A/F to the current throughout the network, each terminal's current can be split into different components generated by the individual internal voltage acting alone in the case of constant parameters of network elements, while the others are nonoperative [46], as shown in Fig. 11.

Step 2. Derive explicit expressions of each current component regarding the internal voltage's A/F.

Concerning general power networks, the integral function is the universal form for the current-voltage instantaneous values relationship [46]. The essential challenge in deriving the network's stimulation-response relationship is how to express the integral function with explicit dependence on the A/F of the internal voltage. The previous section describes the derivation of the current in terms of the internal voltage's A/F using the asymptotic method. This mathematical derivation based on integration by parts can universally accommodate integral functions and will be elaborated with a subsequent example. Therefore, taking terminal k as an example, the current at terminal k contains two types: the current component \mathbf{I}_{s_kk} generated by \mathbf{E}_k and the current component \mathbf{I}_{s_hk} generated by the other $\mathbf{E}_h (h \neq k)$. Moreover, each current component contains two components that are in-phase and orthogonal to its respective internal voltage:

$$\mathbf{I}_k = \sum_{h=1}^n \mathbf{I}_{s_hk} = \sum_{h=1}^n \left(I_{s_hk}^d(t) + jI_{s_hk}^q(t) \right) e^{j\theta_h(t)} \quad (6)$$

where $I_{s_hk}^d(t)$ is parallel to \mathbf{E}_h , $I_{s_hk}^q(t)$ is orthogonal to \mathbf{E}_h , and $\theta_h(t)$ is the phase of \mathbf{E}_h . The current components $I_{s_hk}^d(t)$ and $I_{s_hk}^q(t)$ are explicit expressions of $E_h(t)$ and $\omega_h(t)$.

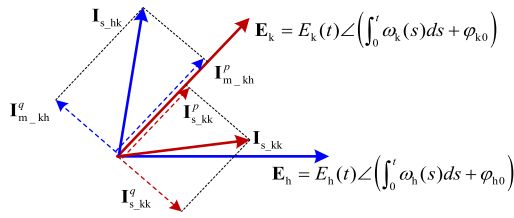


FIGURE 12. Relationships of voltages and current rotation vectors.

Step 3. Decompose the time-varying A/F current into the active/reactive currents based on the internal voltage.

As shown in Fig. 12, each current I_{s_hk} time-varying A/F in (6) is split into components of in-phase and orthogonal to E_k . Thus, the active/reactive current at terminal k consists of two types of components: the active and reactive current self-components $I_{s_kk}^P(t)/I_{s_kk}^Q(t)$ generated by E_k acting alone on the electric network and the active and reactive current mutual-components $I_{m_kh}^P(t)/I_{m_kh}^Q(t)$ generated by the other internal voltage E_h . The $I_{m_kh}^P(t)/I_{m_kh}^Q(t)$ is as follows:

$$\begin{cases} I_{m_kh}^P(t) = I_{s_hk}^d(t) \cos \delta_{kh}(t) + I_{s_hk}^q(t) \sin \delta_{kh}(t) \\ I_{m_kh}^Q(t) = I_{s_hk}^d(t) \sin \delta_{kh}(t) - I_{s_hk}^q(t) \cos \delta_{kh}(t) \end{cases} \quad (7)$$

where $\delta_{kh}(t) = \int_0^t (\omega_k(\tau) - \omega_h(\tau))d\tau + \varphi_{k0} - \varphi_{h0}$.

Step 4. Obtain explicit expression of the network terminal's active/reactive power regarding the internal voltage's A/F.

The self/mutual components of active/reactive current multiplied by $E_k(t)$ equal the self/mutual components of active/reactive power. They are added to obtain the P_k/Q_k (8), as shown at the bottom of the next page, where P_{s_kk}/Q_{s_kk} represents the active/reactive power self components, and P_{m_kh}/Q_{m_kh} represents the mutual components of active/reactive power. Based on the above steps, the terminal power P_k and Q_k are expressed concerning $E_h(t)$ and $\omega_h(t)$, where $h=1, \dots, n$.

2) THE STIMULATION-RESPONSE RELATIONSHIP OF MULTI-TERMINAL ELECTRIC NETWORK

In the network of power systems, there are a number of high-voltage transmission lines and transformers, etc., that are primarily inductive. The inductive network composed of these components is the representative form generally used in system analysis and also a necessary basis for studying the mechanism of dynamic problems. This network is used to illustrate the derivation of the multi-terminal stimulation-response relationships. The line current's instantaneous value is related to the nodal voltage's instantaneous value as follows:

$$\begin{cases} [I_S] = [B_S] \cdot \int_0^t [E_S] d\tau + [B_{ST}] \cdot \int_0^t [U_T] d\tau \\ \mathbf{0} = [B_{TS}] \cdot \int_0^t [E_S] d\tau + [B_T] \cdot \int_0^t [U_T] d\tau \end{cases} \quad (9)$$

where the direction of current flowing into the electric network is specified as the positive direction. $[I_S]$ is the column vector of currents flowing from the equipment to

the electric network, and $[E_S]$ is the column vector of the equipment's internal voltages. $[U_T]$ denotes the column vector composed of network nodal voltages. $[B]$ is the network parameter matrix. The nondiagonal element of the i -th row and j -th column in $[B]$ corresponds to the reciprocal of the parameter of the line connecting the i -th node and j -th node, and the diagonal element of $i=j$ is equal to the sum of the reciprocal of the line parameter connected to node i . $[B_S]$ is a matrix of parameters for the direct connection lines of internal voltage, $[B_{ST}]$ and $[B_{TS}]$ are matrices of parameters of the interconnecting lines between internal voltage and busbar, and $[B_T]$ is a matrix consisting of parameters of interconnecting lines between network nodes. With (9), we obtain

$$[I_S] = [B_{equ}] \cdot \int_0^t [E_S] d\tau \quad (10)$$

where $[B_{equ}] = [B_S] - [B_{ST}][B_T]^{-1}[B_{TS}]$. The instantaneous values of the currents in (10) are equal to the integral of the instantaneous value of the internal voltage over time. The element of the k -th row and h -th column in $[B_{equ}]$ is $B_{kh} = -1/L_{kh}$ and $L_{kh} = L_{hk}$. Using (10), the current at terminal k can be expressed as follows:

$$I_k = \sum_{h=1}^n \left(B_{kh} \int_0^t E_h(\tau) d\tau \right) = \sum_{h=1}^n I_{s_hk} \quad (11)$$

Based on the asymptotic method, it can be derived as below,

$$I_{s_hk} = \sum_{b=1}^{\infty} \left[(-1)^b A_{hk_2b} + j(-1)^b A_{hk_2b-1} \right] \cdot e^{j\theta_h(t)} \quad (12)$$

where,

$$A_{hk_1} = \frac{E_h(t)}{\omega_h(t)L_{kh}}, A_{hk_2} = -\frac{A'_{hk_1}}{\omega_h(t)}, \dots, \\ A_{hk_b} = -\frac{A'_{hk_b-1}}{\omega_h(t)}, \dots$$

Each component of I_k can be split into two components, in-phase and orthogonal to E_k , which correspond to the active and reactive currents. The derivation is not repeated here. Hence, the explicit expressions of the active/reactive power component in (8) for terminal k are as follows (13), shown at the bottom of the next page.

IV. CHARACTERISTICS ANALYSIS OF THE NETWORK'S STIMULATION-RESPONSE RELATIONSHIP IN THE SYSTEM DYNAMICS

To build an intuitive understanding of the characteristics of the network in power system dynamic processes, this section presents an approximation of the network's stimulation-response relationship for the case of a relatively slow changing rate of A/F. With this relationship, several observations are obtained, especially the physical mechanism of the terminal active/reactive power generation in relation to

the internal voltage's time-varying A/F, including its potential impact on the evolution of system dynamics.

A. BASIC CHARACTERISTICS AND SIMPLIFICATION OF THE NETWORK'S RELATIONSHIP

The original expressions of the network's relationship between the internal voltage's time-varying A/F and active/reactive power in (13) include the derivative of the internal voltage's amplitude divided by its frequency and the trigonometric function of the integration of the internal voltages' frequency difference. The faster changes in the A/F lead to larger variations in power asymptotic expansion terms due to the change rate of the A/F. In this way, the network's relationship can be examined based on the time-varying characteristics of the A/F.

In scenarios involving slow changes in the internal voltage's A/F, such as the power system's electromechanical timescale dynamics, the first term of (3) is much larger than the sum of the subsequent terms. The first term can approximate the current. The relationship between voltage and current of line k-h can be geometrically illustrated in Fig. 13 (a), where the line current \mathbf{I}_{kh} is synthesized by \mathbf{I}_{s_kh} and \mathbf{I}_{s_hk} . The angle difference between \mathbf{I}_{kh} and the line voltage is as follows:

$$\alpha_{kh}(t) = \text{Arg} \left(\frac{\mathbf{u}_{kh}}{\mathbf{I}_{kh}} \right) = \text{Arg} \left(j \frac{(\mathbf{E}_k - \mathbf{E}_h) L_{kh}}{\mathbf{E}_k / \omega_k(t) - \mathbf{E}_h / \omega_h(t)} \right) \quad (14)$$

It is clear that only when $\omega_k(t) = \omega_h(t)$, the $\alpha_{kh}(t) = \pi/2$, and the line current vector is perpendicular to the voltage vector. However, in system dynamics, the frequencies of different internal voltages are time-varying and unequal, and $\alpha_{kh}(t)$ is not constant at $\pi/2$. This means that \mathbf{I}_{kh} is not

perpendicular to the voltage \mathbf{u}_{kh} of the line k-h. In this case, the network's stimulation-response relationships are simplified as

$$\begin{aligned} P_k + jQ_k &= \frac{3}{2} \sum_{h=1, h \neq k}^n \frac{E_k(t)E_h(t)}{\omega_h(t)L_{kh}} \sin \delta_{kh}(t) \\ &+ \frac{3j}{2} \sum_{h=1, h \neq k}^n \left(\frac{E_k^2(t)}{\omega_k(t)L_{kh}} - \frac{E_k(t)E_h(t)}{\omega_h(t)L_{kh}} \cos \delta_{kh}(t) \right) \end{aligned} \quad (15)$$

It contains the algebraic relationship of each internal voltage's A/F and the phase difference generated by the integration of the frequency difference. The mathematical expression based on the first term of the current expansion provides an approximate relationship, denoting the network's simplified relationship. This helps in comprehending the characteristics of the network's terminal active/reactive power change with the internal voltage's time-varying A/F.

As for the steady-state operation, the A/F of the internal voltage is constant, and (15) reduces to the usual "phasor" model [47]. The voltage and current are represented by the phasor denoted with a "." superscript and depicted with a phasor diagram, as shown in Fig. 13 (b). \dot{I}_{kh} is always perpendicular to \dot{u}_{kh} . The active/reactive power at terminal k of the network is,

$$\begin{aligned} P_k + jQ_k &= \frac{3}{2} \sum_{h=1, h \neq k}^n \left(\frac{E_k E_h}{\omega_0 L_{kh}} \sin \delta_{kh} + j \frac{E_k^2 - E_k E_h \cos \delta_{kh}}{\omega_0 L_{kh}} \right) \end{aligned} \quad (16)$$

$$\begin{aligned} P_k + jQ_k &= P_{s_kk} + \sum_{h=1, h \neq k}^n P_{m_kh} + j \left(Q_{s_kk} + \sum_{h=1, h \neq k}^n Q_{m_kh} \right) \\ &= \frac{3}{2} E_k(t) \left[I_{s_kk}^P(t) + j I_{s_kk}^Q(t) + \sum_{h=1, h \neq k}^n \left(I_{m_kh}^P(t) + j I_{m_kh}^Q(t) \right) \right] \\ &= \frac{3}{2} E_k(t) \left[I_{s_kk}^d(t) + \sum_{h=1, h \neq k}^n \left(I_{s_hk}^d(t) \cos \delta_{kh}(t) + I_{s_hk}^q(t) \sin \delta_{kh}(t) \right) \right] \\ &+ j \frac{3}{2} E_k(t) \left[-I_{s_kk}^q(t) + \sum_{h=1, h \neq k}^n \left(I_{s_hk}^d(t) \sin \delta_{kh}(t) - I_{s_hk}^q(t) \cos \delta_{kh}(t) \right) \right] \end{aligned} \quad (8)$$

$$\begin{cases} P_{s_kk} = \frac{3E_k(t)}{2} \sum_{b=1}^{\infty} (-1)^b A_{kk_2b}, Q_{s_kk} = \frac{3E_k(t)}{2} \sum_{b=1}^{\infty} (-1)^{b+1} A_{kk_2b-1} \\ P_{m_kh} = \frac{3E_k(t)}{2} \sum_{b=1}^{\infty} (-1)^b (A_{hk_2b} \cos \delta_{kh}(t) + A_{hk_2b-1} \sin \delta_{kh}(t)) \\ Q_{m_kh} = \frac{3E_k(t)}{2} \sum_{b=1}^{\infty} (-1)^{b-1} (A_{hk_2b-1} \cos \delta_{kh}(t) - A_{hk_2b} \sin \delta_{kh}(t)) \end{cases} \quad (13)$$

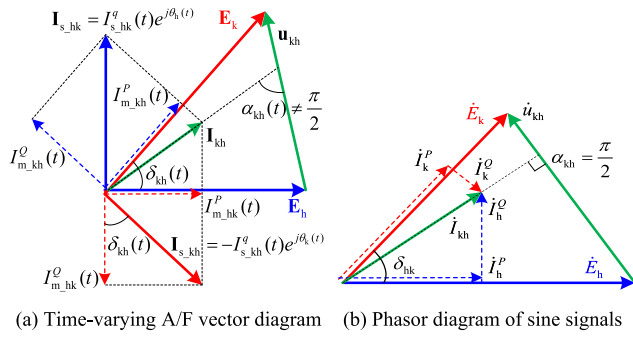


FIGURE 13. Geometrical relationships between voltages and currents.

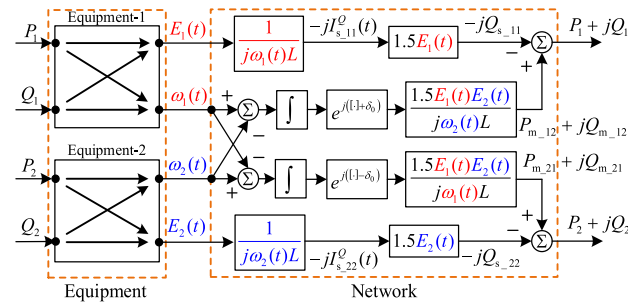


FIGURE 14. Block diagram of the 2-machines system.

Although this static network relationship is derived under the steady state, it is often used in power system dynamic analysis with the “quasi-steady state” assumption, assuming the frequency is constant. In literature [1], the static network relationship is viewed as if the network directly passes from one steady state to another when subjected to disturbances. However, even in the system’s electromechanical timescale dynamics, we observe several differences in the characteristics of the network’s simplified relationship from the familiar static network relationship, potentially impacting the system’s dynamic process.

B. CHARACTERISTIC DISTINCTIONS OF DIFFERENT RELATIONSHIPS OF NETWORK IN SYSTEM’S ELECTROMECHANICAL TIMESCALE DYNAMICS

Both (15) and (16) contain the algebraic relationship of the internal voltage’s amplitude, but the frequency relationship is reflected differently. While the synchronization problem of the power system is closely related to the internal voltage’s frequency dynamics [2], this section elaborates on this issue using the 2-machines system in Fig. 14.

As shown in Fig. 14, when the frequencies of the two equipment’s internal voltages are not equal, the integration of frequency difference is not zero. Consequently, the phase difference changes, and the exchanged active/reactive power between the equipment and the network varies. To balance the output and the command of the active power, the equipment regulates its internal voltage’s frequency. For instance, the synchronous machine changes its rotor speed according to the imbalanced active power, and the internal voltage’s frequency varies as the frequency is directly coupled with

the rotor speed. Similarly, the reactive power change drives the equipment to regulate the internal voltage’s frequency variation through its control coupling path that links reactive power to frequency. For instance, the internal control strategies of the wind turbine have coupling paths to affect the internal voltage’s frequency [20]. If there are no coupling paths in electric equipment, changes in reactive power still affect the amplitude of the internal voltage by control and then affect the active power of the network. Then, the control of the equipment adjusts the internal voltage’s frequency. The above processes last until all of the equipment’s frequencies reach synchronous, and thus, the phase difference no longer changes.

With the above considerations, the system’s synchronous operation is, by nature, a closed-loop regulation process between the frequency of the equipment’s internal voltage and the terminal active/reactive power of the network. This process is closely related to the whole system’s power (energy) balancing. It is clear that the variations in the electric network terminal’s power caused by the frequencies of the internal voltages act as an important driver in the evolution of the system dynamics. Therefore, based on Fig. 14, several observations for the properties of the network’s relationships, including their potential impact on the evolution of system dynamics, are as follows:

1) The terminal power explicitly contains both self and mutual components with an inherent relationship expressed in terms of the time-varying A/F of different internal voltages. Since the current contains components excited by different internal voltages, its generated terminal power has both self and mutual components produced by different internal voltages. Therefore, the terminal power has self and mutual components, and their regulation is inherently driven by the time-varying A/F of different internal voltages under the equipment’s control. This mechanism is reflected in the network’s stimulation–response relationships obtained in this paper.

2) Changes in the electric network’s terminal power drive the evolution of the system’s closed-loop regulation in dynamics. In contrast to the static network relationships, there is the frequency algebraic relationship of the different terminal’s voltages in the self/mutual components of the network power. It has instantaneous impacts on the reactive power self-components at the same terminal and the active/reactive power mutual-components at other terminals. Different network relationships will lead to different recognitions of potential impacts on system dynamics.

3) The active power at both terminals of the inductive line is imbalanced, so as is the reactive power, as shown in Fig. 14. It reflects the physical property of active power and reactive power consumption on the inductive line during disturbances, which is unforeseen from the common physical understanding of only reactive power consumption on the inductive line under the static network relationships. In particular, the electric network contains a large number of inductive components, emphasizing the importance of

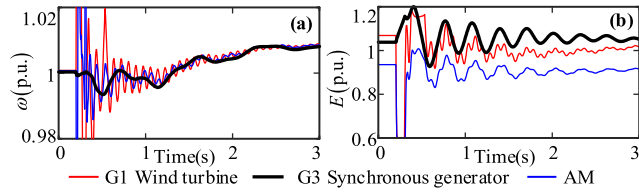


FIGURE 15. Details of simulation results under case 1 large disturbance: (a) Internal voltage's frequency; (b) Internal voltage's amplitude.

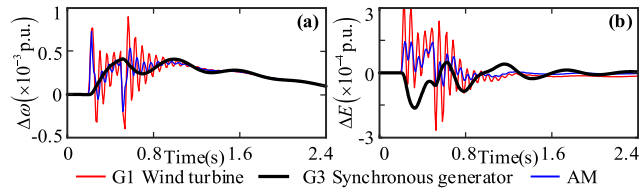


FIGURE 16. Details of simulation results under case 2 small disturbance: (a) Internal voltage's frequency; (b) Internal voltage's amplitude.

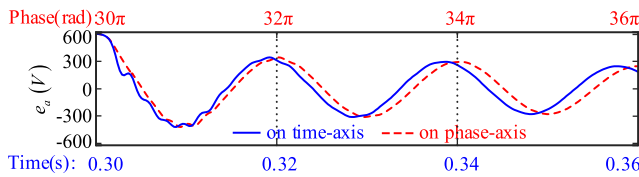


FIGURE 17. The AC waveform of the G1 internal voltage on the phase-axis and the time-axis.

active and reactive power consumption characteristics in the power system dynamic process. It also provides the relationship between the equipment terminal power (energy) and the network's internally consumed power (energy). These physical characteristics and relationships are the indispensable basis for understanding the balance of power and energy in the power system dynamics.

V. SIMULATION STUDY FOR THE NETWORK'S RELATIONSHIP

In this section, the simulation in a multi-machine system, shown in the Appendix, will help further understand the network relationship and its characteristics.

A. NETWORK'S TERMINAL POWER GENERATION IN RELATION TO THE TIME-VARYING A/F

Two representative scenarios of the large and small disturbances are taken for illustration, which are as follows:

Case 1: A three-phase symmetric fault occurs at Bus-8 at 0.2 s; then, line 8-9 breaks at 0.3 s.

Case 2: A fluctuation disturbance of 5 MW at Bus-5 lasting 0.3s occurs at 0.2 s.

Fig. 15 and Fig. 16 depict the simulation results for the A/F of different equipment, presenting different time-varying characteristics. From the red and blue lines in Fig.15 (a)-(b), the rapid changes in instantaneous A/F of the wind turbine and the asynchronous machine (AM) are observed with a wider range of variations than the black lines of the G3 during the large disturbance. The A/F of the

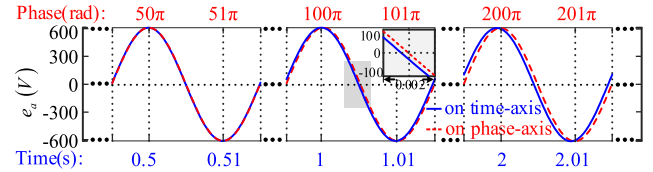


FIGURE 18. The AC waveform of the G1 internal voltage on the phase-axis and the time-axis.

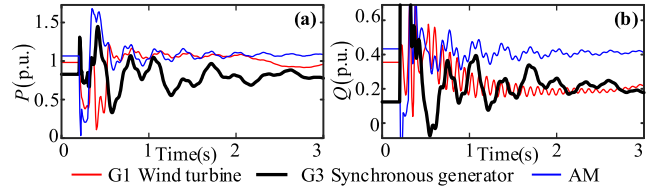


FIGURE 19. Details of simulation results under case 1 large disturbance: (a) The network terminal active power; (b) The network terminal reactive power.

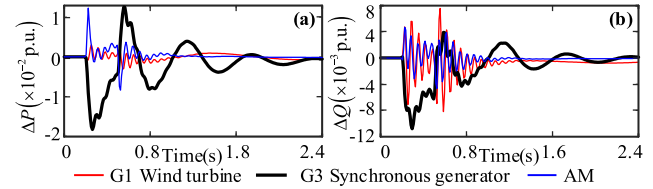


FIGURE 20. Details of simulation results under case 2 small disturbance: (a) The network terminal active power; (b) The network terminal reactive power.

internal voltage of the wind turbine and the AM contains high-frequency to low-frequency fluctuations when subjecting the small disturbance, shown in the red and blue lines of Fig. 16 (a)-(b). Compared with the relatively slow changes in the instantaneous A/F of the SG's internal voltage, the internal voltage's A/F of the wind turbine and the AM present more complex characteristics with rapid changes and wide-range fluctuations.

The AC waveforms of the internal voltage of G1 are shown in Fig. 17 and Fig. 18. Compared with the waveform on the phase-axis, the time-varying A/F with fast and slow changes makes the AC waveform on the time-axis appear like harmonics inside and at different alternating times. Such voltages with complex time-varying A/F generate the terminal power, as shown in Fig. 19 and Fig. 20. It is apparent that the active/reactive power of G3 exhibits variations that include rapid changes and fluctuations ranging from high to low frequency, whose characteristics similar to those of the wind turbine (red lines) and the AM (blue lines). These fluctuations differ from the time-varying A/F characteristics of G3 (as shown in Fig. 15 and Fig. 16). Clearly, there is a relationship that makes the G3's output power behave differently from the itself time-varying A/F characteristics.

It is known from the previous section that the power at any given terminal of an electric network is generated by the connected internal voltage together with its output current containing components separately dependent on itself and the others. Thus, the terminal power has both self

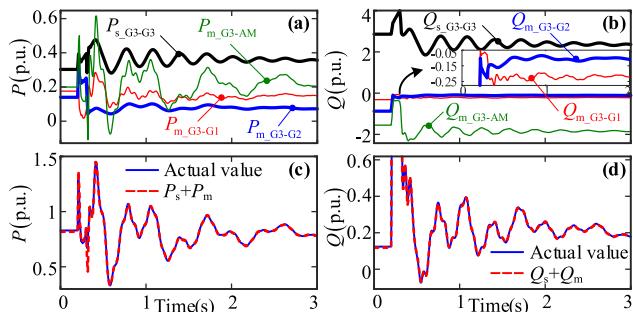


FIGURE 21. Decomposition of G3 output power under case 1 large disturbance: (a) Active power self/mutual components; (b) Reactive power self/mutual components; (c) G3 output active power; (d) G3 output reactive power.

and mutual components with different physical meanings in relation to time-varying A/F of different internal voltages. We take the power of G3 as an example, where the subscript “G3-X” of power denotes the component of the G3 power generation related to the current separately excited by equipment-X. The summation of the power’s self/mutual components is consistent with the directly measured values, as shown in (c)-(d) of Fig. 21 and Fig. 22. When subjected to the large disturbance, as shown in Fig. 21 (a)-(b), the black lines of P_{s_G3-G3}/Q_{s_G3-G3} and the blue lines of P_{m_G3-G2}/Q_{m_G3-G2} exhibit slow changes. In contrast, the green lines of P_{m_G3-AM}/Q_{m_G3-AM} and the red lines of P_{m_G3-G1}/Q_{m_G3-G1} have rapid changes with a wide range and after 2 s, exhibit slow fluctuations. As for the small disturbance shown in Fig. 22 (a)-(b), the green lines of P_{m_G3-AM}/Q_{m_G3-AM} and the red lines of P_{m_G3-G1}/Q_{m_G3-G1} present fluctuating components with high-frequency to low-frequency. The self and mutual components of the terminal power generated by SGs exhibit only slow changes, while the mutual-components of the terminal power formed by the wind turbine G1 with the AM exhibit variations in different degrees. Therefore, the results indicate that the time-varying A/F of each equipment’s internal voltage generates the self/mutual components to form the network terminal’s power and determine its variation features.

Furthermore, the self and mutual components of the terminal power separate the factors of one equipment’s output power affected by other equipment. This can help provide insight into how different equipment interacts with each other via the network to cause system instability. For example, when the SG’s model is replaced by multi-mass in this simulation, due to the internal voltage’s A/F of the wind turbine G1 containing sub-synchronous frequency range dynamics, the SG with the wind turbine forms the mutual component in terminal active power may cause torsional vibration of the shaft. When subjected to a large disturbance, the A/F of the AM internal voltage changes rapidly with large magnitude and affects the mutual-components of the SG power, resulting in the acceleration or deceleration of the SG’s rotor.

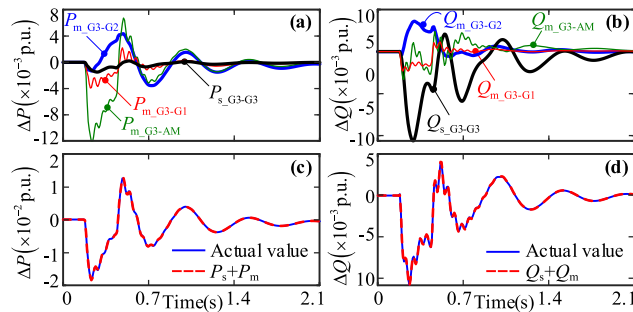


FIGURE 22. Decomposition of G3 output power under case 2 small disturbance: (a) Active power self/mutual components; (b) Reactive power self/mutual components; (c) G3 output active power; (d) G3 output reactive power.

As shown in the above simulation results, the instantaneous A/F of varied equipment’s internal voltage presents complex time-varying characteristics. It is clear that the corresponding AC waveform cannot be treated as a sine signal with constant A/F. The inherent properties of the network’s stimulation–response relationship determine the characteristics of the terminal power variation. Moreover, the terminal power has self and mutual components with different physical meanings that reflect time-varying A/F of multiple internal voltages.

B. CHARACTERISTICS OF THE NETWORK’S RELATIONSHIPS

This section examines the basic characteristics of the network’s stimulation–response relationships via simulation. The simulation is based on the 3-machine 9-bus system and considers the wind speeds of the wind turbine changing from 10 m/s to 12 m/s at 1 s and then back to 10 m/s at 3.5 s. Waveforms at the terminals of line 4-5 are measured and shown in Fig. 23, along with the waveforms of the established network’s simplified relationship and the static network relationship are also presented.

Fig. 23 (a) shows that the time-varying instantaneous frequencies at nodes 4 and 5 are unequal. The integration of the frequency difference generates the phase difference change of nodes 4-5 in Fig. 23 (b). Fig. 23 (c) gives the waveform of the phase difference between the line voltage and the line current. Fig. 23 (d)-(h) shows the waveforms of active/reactive power obtained through the network’s simplified relationships (red dashed lines), the actual measured waveforms (blue lines), and the static network relationships (black dashed lines).

Fig. 23 (c) clearly shows that the phase difference between the voltage and current is not 90 degrees, which means the time-varying A/F voltage generates not only an orthogonal but also an in-phase current component. This characteristic is not reflected in the static network relationship. So, the active power measured at nodes 4 and 5 will be different, as shown in Fig. 23 (d). In Fig. 23 (e)-(h), it can be seen that the waveforms obtained through the network’s simplified relationships are consistent with the actual measured waveforms. In contrast, the static network

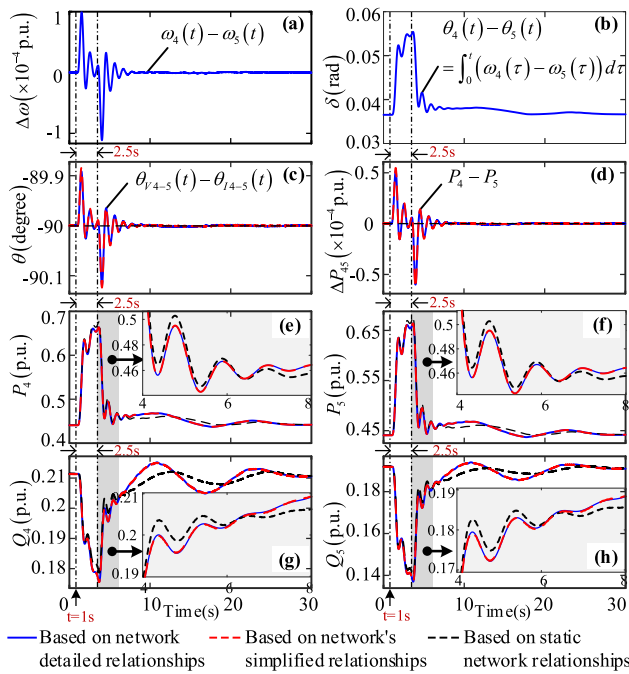


FIGURE 23. Simulation results of different network's relationships: (a) Frequency difference between nodes 4 and 5; (b) The phase difference of nodes 4–5; (c) Phase difference between the line-voltage u_{45} and line-current i_{45} ; (d) Active power difference $P_4 - P_5$; (e) Node 4 output active power P_4 ; (f) Node 5 received active power P_5 ; (g) Node 4 output reactive power Q_4 ; (h) Node 5 received reactive power Q_5 .

relationships exhibit different variations in power. It can be found that the occurrence of the physical phenomena is because the time-varying frequency has an instantaneous impact on the magnitude of power based on the (15) and (16).

The simulation results validate the observed characteristics. When a time-varying A/F voltage is applied to an inductive component, an in-phase current component will be produced. Thus, there is a property of active/reactive power consumption on the inductive line in dynamics. Meanwhile, it indicates that the internal voltage's time-varying frequency has an instantaneous impact on the self-components of the reactive power at the same terminal and the mutual-components of the active/reactive power at the other terminals. However, these physical properties are unobservable based on the static network relationships, which use the phase difference as a state to quantify the power variations instead of the frequency and hinder insight into its potential impact on the system dynamics.

VI. CONCLUSION AND DISCUSSIONS

Based on recognizing the inherent time-varying A/F of equipment's internal voltage in the system's dynamic processes, to serve for the power system analysis, the relationship of the electric network between the internal voltage's time-varying A/F stimulation and the active/reactive power response is established and studied in this paper. The main conclusions are summarized as follows:

1) It elaborates in detail the method of establishing the relationship based on internal voltage's A/F and active/reactive power. It also obtains the explicit original expressions of the active/reactive power with the integration by parts expansion. The network relationship retains the key information of the A/F and active/reactive power required for the system dynamics analysis.

2) Based on the explicit original expressions of the network relationships, a physical characteristic that is unforeseen from the common understanding is observed. A time-varying A/F internal voltage, when applied to an inductive component, generates not only an orthogonal but also an in-phase current component, which means it will produce both reactive and active power.

3) A network simplified relationship for the case of a relatively slow changing rate of A/F and several unusual observations are obtained. Since the power at any given terminal in a network is generated by the connected internal voltage together with its output current containing components separately dependent on itself and the others, each terminal power has both self and mutual components with different physical meanings in relation to time-varying A/F of multiple internal voltages. Meanwhile, the time-varying frequency of the internal voltage, in addition to the integral relationship, has an algebraic relationship with the power that is characterized by instantaneous impacts on the same terminal power's self-components and on other terminal power's mutual components. In addition, the active/reactive power at both terminals of the inductive line is imbalanced, which means the active/reactive power is consumed on the inductive line in dynamics.

It is clear that the established relationship of the electric network and its unforeseen basic characteristics will strongly influence the analysis and understanding of the system dynamic problems. It is believed that it will also stimulate people to recognize the necessity of the related work. Continued in-depth research is necessary around the characteristics of the network:

Due to the multiple timescale control regulation of converter-interfaced equipment, multi-timescale dynamics arise in the internal voltage's A/F during disturbances. Although the original explicit expressions of the network relationships cover various scenarios of the time-varying A/F with different characteristics, the expressions are somewhat complicated and need further investigations on the expressions retaining finite terms of the network relationship for the system analysis under disturbances with different characteristics and the changing rate of the A/F impact on the system dynamics.

The active/reactive power consumption of the inductive components observed in this paper is an important issue for understanding power and energy balancing in system dynamics. The physical characteristics and their impacts on the system dynamics need further study.

The present work is expected to lay a foundation for further understanding of the physics and corresponding analytics

of the network and, ultimately, for practical application purposes.

APPENDIX

The simulation system evolved from the WSCC 3-machines 9-bus system, as shown in Fig. 24, and simulated in MATLAB/Simulink. G1 is replaced with a GE Type-4 wind turbine, and the load at bus-6 is replaced with an asynchronous machine. The parameters are shown below. The waveforms of each piece of equipment are given per unit with respect to the rated voltage and 100 MVA base.

- 1) The wind turbine parameters are as shown in the Table 1.
- 2) Static excitation control parameters

$$\Delta E_{fd} = \frac{K_A}{1 + T_A s} (V_t^{\text{ref}} - V_t) \quad (17)$$

where G2: $K_A = 150$, $T_e = 0.02$; G3: $K_A = 200$, $T_e = 0.02$.

- 3) The wind turbine parameters are as shown in the Table 2.

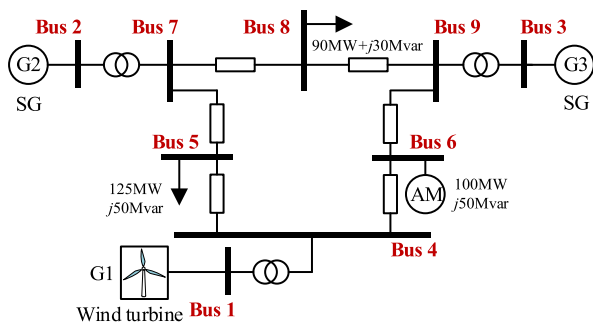


FIGURE 24. The 3-machine 9-bus system.

TABLE 1. Parameters of asynchronous machine.

Description	Values
Nominal power, voltage	$S_n=137$ MW, $V_n=400$ V
Stator resistance and inductance (p.u.)	$L_s=0.0435$, $R_s=0.0425$
Rotor resistance and inductance (p.u.)	$L_r=0.0329$, $R_r=0.0739$
Mutual inductance (p.u.)	$L_m=2.9745$
Inertia constant	$H=0.6$ s

TABLE 2. Controller parameters values.

Description	Values
Grid-side nominal power, voltage, and number of wind turbines	$S_n=2$ MW, $V_n=690$ V, $N=50$
DC bus voltage regulator (p.u.)	$k_{dc_p}=0.6$, $k_{dc_i}=10$
Grid-side converter current regulator (p.u.)	$k_{i_p}=0.8$, $k_{i_i}=30$
Grid-side converter voltage regulator (p.u.)	$k_{v_i}=2$
Phase Locked Loop (p.u.)	Case 1: $k_{pll_p}=65$, $k_{pll_i}=6020$ Case 2: $k_{pll_p}=120$, $k_{pll_i}=6020$
Speed regulator (p.u.)	$k_{w_p}=5$, $k_{w_i}=1$

REFERENCES

- [1] P. S. Kundur, *Power System Dynamics and Stability, Power System Stability and Control*, 3rd ed. Boca Raton, FL, USA: CRC Press, 2017.

- [2] L. L. Grigsby, *Power System Stability and Control*. Boca Raton, FL, USA: CRC Press, 2012.
- [3] N. Kamel and J. W. Glotfelty, (2003). *Interim Report: Causes of the August 14th Blackout in the United States and Canada*. [Online]. Available: <https://www.energy.gov/sites/prod/files/oeprod/DocumentsandMedia/BlackoutFinal-Web.pdf>
- [4] Union for the Coordination of Transmission of Electricity. (2007). *Final Report-System Disturbance on 4 November 2006*. [Online]. Available: <https://eepublicdownloads.entsoe.eu/clean-documents/pre2015/publications/ce/otherreports/IC-Interim-Report-20061130.pdf>
- [5] NERC Task. *1,200 MW Fault Induced Solar Photovoltaic Resource Interruption Disturbance Report*. [Online]. Available: <https://www.nerc.com/pa/trm/ea/Pages/1200-MW-Fault-Induced-Solar-Photovoltaic-Resource-Interruption-Disturbance-Report.aspx>
- [6] AEMO. (2021). *West Murray Zone Intermittent Power System Oscillations*. [Online]. Available: <https://www.aemo.com.au/energy-systems/electricity/national-electricity-market-nem/system-operations/power-system-oscillations>
- [7] Y. Cheng, L. Fan, J. Rose, S.-H. Huang, J. Schmall, X. Wang, X. Xie, J. Shair, J. R. Ramamurthy, N. Modi, C. Li, C. Wang, S. Shah, B. Pal, Z. Miao, A. Isaacs, J. Mahseredjian, and J. Zhou, "Real-world subsynchronous oscillation events in power grids with high penetrations of inverter-based resources," *IEEE Trans. Power Syst.*, vol. 38, no. 1, pp. 316–330, Jan. 2023, doi: [10.1109/TPWRS.2022.3161418](https://doi.org/10.1109/TPWRS.2022.3161418).
- [8] X. Yuan and S. Wang, "Operating-point identification from dimensions of alternating signal based on the incremental iterative mapping mechanism for analyzing dynamics of AC systems," *CSEE J. Power Energy Syst.*, pp. 1–10, 2023. [Online]. Available: <https://ieeexplore.ieee.org/document/10106197>
- [9] *IEEE Standard Definitions for the Measurement of Electric Power Quantities under Sinusoidal, Non-Sinusoidal, Balanced, or Unbalanced Conditions*, IEEE Standard 1459-2000, 2000, pp. 1–52.
- [10] *IEEE/IEC International Standard—Measuring Relays and Protection Equipment—Part 118-1: Synchrophasor for Power Systems—Measurements*, Standard IEC/IEEE 60255-118-1, Dec. 2018, doi: [10.1109/IEEESTD.2018.8577045](https://doi.org/10.1109/IEEESTD.2018.8577045).
- [11] A. M. Muscas and F. Ponci, *Phasor Measurement Units and Wide Area Monitoring Systems: From the Sensors to the System*. Amsterdam, The Netherlands: Elsevier, 2016, pp. 1–286.
- [12] J. R. Carson and T. C. Fry, "Variable frequency electric circuit theory with application to the theory of frequency-modulation," *Bell Syst. Tech. J.*, vol. 16, no. 4, pp. 513–540, Oct. 1937, doi: [10.1002/j.1538-7305.1937.tb00766.x](https://doi.org/10.1002/j.1538-7305.1937.tb00766.x).
- [13] S. Sandoval and P. L. De Leon, "The instantaneous spectrum: A general framework for time-frequency analysis," *IEEE Trans. Signal Process.*, vol. 66, no. 21, pp. 5679–5693, Nov. 2018, doi: [10.1109/TSP.2018.2869121](https://doi.org/10.1109/TSP.2018.2869121).
- [14] F. Milano, "A geometrical interpretation of frequency," *IEEE Trans. Power Syst.*, vol. 37, no. 1, pp. 816–819, Jan. 2022, doi: [10.1109/TPWRS.2021.3108915](https://doi.org/10.1109/TPWRS.2021.3108915).
- [15] M. Zhao, X. Yuan, and J. Hu, "Modeling of DFIG wind turbine based on internal voltage motion equation in power systems phase-amplitude dynamics analysis," *IEEE Trans. Power Syst.*, vol. 33, no. 2, pp. 1484–1495, Mar. 2018, doi: [10.1109/TPWRS.2017.2728598](https://doi.org/10.1109/TPWRS.2017.2728598).
- [16] *IEEE Guide for Synchronous Generator Modeling Practices and Parameter Verification With Applications in Power System Stability Analyses*, IEEE Standard 1110-2019, Mar. 2020, pp. 1–92.
- [17] X. Gong, X. Yuan, J. Hu, and S. Wang, "Modeling of VSC with active/reactive current excitation and internal voltage response for analyzing amplitude/frequency modulation dynamics of the grid," *CSEE J. Power Energy Syst.*, pp. 1–9, 2023. [Online]. Available: <https://ieeexplore.ieee.org/document/10106195>, doi: [10.17775/CSEEJPES.2022.00560](https://doi.org/10.17775/CSEEJPES.2022.00560).
- [18] E. R. C. Da Silva and M. E. Elbuluk, "Fundamentals of power electronics," in *Power Electronics for Renewable and Distributed Energy Systems: A Sourcebook of Topologies, Control and Integration*, S. Chakraborty, Ed. London, U.K.: Springer, 2013, pp. 7–59.
- [19] K. K. Sen and M. L. Sen, *Introduction to FACTS Controllers: Theory, Modeling, and Applications*. Hoboken, NJ, USA: Wiley, 2009, pp. 1–523.
- [20] J. Huang, X. Yuan, and S. Wang, "Power-imbalance stimulation and internal-voltage response relationships based modeling method of PE-interfaced devices in DC voltage control timescale," *IEEE Access*, vol. 11, pp. 105214–105224, 2023, doi: [10.1109/ACCESS.2023.3316015](https://doi.org/10.1109/ACCESS.2023.3316015).

- [21] M. Wan, X. Yuan, and J. Hu, "Relationships of internal voltage dependence on power imbalance illustrating characteristics and roles in system dynamics of inertial-controlled DFIG-based wind turbines," *CSEE J. Power Energy Syst.*, pp. 1–10, 2022. [Online]. Available: <https://ieeexplore.ieee.org/document/9770544>, doi: [10.17775/CSEE-JPES.2021.05250](https://doi.org/10.17775/CSEE-JPES.2021.05250).
- [22] A. Iserles and S. P. Nørsett, "On quadrature methods for highly oscillatory integrals and their implementation," *BIT Numer. Math.*, vol. 44, no. 4, pp. 755–772, Dec. 2004, doi: [10.1007/s10543-004-5243-3](https://doi.org/10.1007/s10543-004-5243-3).
- [23] D. Huybrechs and S. Vandewalle, "On the evaluation of highly oscillatory integrals by analytic continuation," *SIAM J. Numer. Anal.*, vol. 44, no. 3, pp. 1026–1048, Jan. 2006, doi: [10.1137/050636814](https://doi.org/10.1137/050636814).
- [24] E. M. Stein and R. Shakarchi, "Functional analysis: Oscillatory integrals," in *Fourier Analysis, Introduction to Further Topics in Analysis*. Princeton, NJ, USA: Princeton Univ. Press, 2011, pp. 321–408.
- [25] R. S. Elias and M. Stein, *Fourier Analysis: An Introduction*. Princeton, NJ, USA: Princeton Univ. Press, 2003.
- [26] W. G. Heffron and R. A. Phillips, "Effect of a modern amplidyne voltage regulator on underexcited operation of large turbine generators [includes discussion]," *Trans. Amer. Inst. Electr. Eng., III, Power App. Syst.*, vol. 71, no. 3, pp. 692–697, Aug. 1952, doi: [10.1109/AIEEPAS.1952.4498530](https://doi.org/10.1109/AIEEPAS.1952.4498530).
- [27] F. Demello and C. Concordia, "Concepts of synchronous machine stability as affected by excitation control," *IEEE Trans. Power App. Syst.*, vol. PAS-88, no. 4, pp. 316–329, Apr. 1969, doi: [10.1109/TPAS.1969.292452](https://doi.org/10.1109/TPAS.1969.292452).
- [28] E. V. Larsen and D. A. Swann, "Applying power system stabilizers. Part I: General concepts," *IEEE Power Eng. Rev.*, vol. PER-1, no. 6, pp. 62–63, Jun. 1981, doi: [10.1109/MPER.1981.5511615](https://doi.org/10.1109/MPER.1981.5511615).
- [29] R. H. Park and E. H. Bancker, "System stability as a design problem," *Trans. Amer. Inst. Electr. Eng.*, vol. 48, no. 1, pp. 170–193, Jan. 1929, doi: [10.1109/T-AIEE.1929.5055195](https://doi.org/10.1109/T-AIEE.1929.5055195).
- [30] P. M. Anderson, *Analysis of Faulted Power Systems*. Ames, IA, USA: Iowa State Univ. Press, vol. 1973, p. 513.
- [31] C. L. Fortescue, "Transmission stability analytical discussion of some factors entering into the problem," *Trans. Amer. Inst. Electr. Eng.*, vol. 44, pp. 984–1003, Jan. 1925, doi: [10.1109/T-AIEE.1925.5061185](https://doi.org/10.1109/T-AIEE.1925.5061185).
- [32] A. Semlyen, "Analysis of disturbance propagation in power systems based on a homogeneous dynamic model," *IEEE Trans. Power App. Syst.*, vol. PAS-93, no. 2, pp. 676–684, Mar. 1974, doi: [10.1109/TPAS.1974.294030](https://doi.org/10.1109/TPAS.1974.294030).
- [33] R. L. Cresap and J. F. Hauer, "Emergence of a new swing mode in the western power system," *IEEE Power Eng. Rev.*, vol. PER-1, no. 4, p. 72, Apr. 1981, doi: [10.1109/MPER.1981.5511429](https://doi.org/10.1109/MPER.1981.5511429).
- [34] K. P. Nnoli, F. Delic, and S. Kettmann, "Transient dynamics and propagation of voltage and frequency fluctuations in transmission grids," *IEEE Access*, vol. 11, pp. 11307–11328, 2023, doi: [10.1109/ACCESS.2023.3241014](https://doi.org/10.1109/ACCESS.2023.3241014).
- [35] K. Pal Nnoli, S. Kettmann, M. S. Benyeogor, and O. O. Olakanmi, "A dynamic model of realistic Nigerian 330 kV transmission network: A catalyst to realistic grid studies and expansion strategy," in *Proc. Int. Conf. Electr., Comput. Energy Technol. (ICECET)*, Dec. 2021, pp. 1–9.
- [36] P. W. Saumar, B. C. Lesieutre, and M. A. Pai, "Transient algebraic circuits for power system dynamic modeling," *Int. J. Electr. Power Energy Syst.*, vol. 15, no. 5, pp. 315–321, 1993, doi: [10.1016/0142-0615\(93\)90053-P](https://doi.org/10.1016/0142-0615(93)90053-P).
- [37] A. Anon, "Damping representation for power system stability studies," *IEEE Trans. Power Syst.*, vol. 14, no. 1, pp. 151–157, Apr. 1999, doi: [10.1109/59.744507](https://doi.org/10.1109/59.744507).
- [38] H. Yang and X. Yuan, "Power characteristics with excitation of time-varying amplitude-frequency internal voltages during electromechanical dynamic process in power systems," *Proc. CSEE*, vol. 41, no. 9, pp. 3079–3090, May 2021.
- [39] S. M. Kotian and K. N. Shubhanga, "Performance of synchronous machine models in a series-capacitor compensated system," *IEEE Trans. Power Syst.*, vol. 29, no. 3, pp. 1023–1032, May 2014, doi: [10.1109/TPWRS.2013.2292977](https://doi.org/10.1109/TPWRS.2013.2292977).
- [40] J. Belikov and Y. Levron, "Uses and misuses of quasi-static time-varying phasor models in power systems," *IEEE Trans. Power Del.*, vol. 33, no. 6, pp. 3263–3266, Dec. 2018, doi: [10.1109/TPWRD.2018.2852950](https://doi.org/10.1109/TPWRD.2018.2852950).
- [41] D. Groß, M. Colombino, J.-S. Brouillon, and F. Dörfler, "The effect of transmission-line dynamics on grid-forming dispatchable virtual oscillator control," *IEEE Trans. Control Netw. Syst.*, vol. 6, no. 3, pp. 1148–1160, Sep. 2019, doi: [10.1109/TCNS.2019.2921347](https://doi.org/10.1109/TCNS.2019.2921347).
- [42] E. H. Allen and M. D. Ilic, "Interaction of transmission network and load phasor dynamics in electric power systems," *IEEE Trans. Circuits Syst. I, Fundam. Theory Appl.*, vol. 47, no. 11, pp. 1613–1620, Oct. 2000, doi: [10.1109/81.895329](https://doi.org/10.1109/81.895329).
- [43] J. Zaborszky, H. Schattler, and V. Venkatasubramanian, "Error estimation and limitation of the quasi-stationary phasor dynamics," in *Proc. Power Syst. Comput. Conf.*, 1993, pp. 721–729.
- [44] C. L. DeMarco and G. C. Verghese, *Bringing Phasor Dynamics Into the Power System Load Flow*. Washington, DC, USA: IEEE Comput. Soc. Press, 1993, pp. 463–471.
- [45] V. Venkatasubramanian, "Tools for dynamic analysis of the general large power system using time-varying phasors," *Int. J. Electr. Power Energy Syst.*, vol. 16, no. 6, pp. 365–376, Dec. 1994, doi: [10.1016/0142-0615\(94\)90023-X](https://doi.org/10.1016/0142-0615(94)90023-X).
- [46] C. Satyanarayana, "Applied graph theory: Graphs and electrical networks," *Proc. IEEE*, vol. 66, no. 10, pp. 1299–1300, Feb. 1978.
- [47] C. P. Steinmetz, "Complex quantities and their use in electrical engineering," in *Proc. Int. Electr. Congr.*, 1893, pp. 33–75.



RONGXIN SUN (Student Member, IEEE) received the B.Eng. degree from the School of Electrical and Engineering, Huazhong University of Science and Technology (HUST), Wuhan, China, in July 2016. He is currently pursuing the Ph.D. degree with the State Key Laboratory of Advanced Electromagnetic and Technology, School of Electrical and Electronic Engineering, HUST.

His current research interests include dynamics of power electronics dominated large power systems, including the stability and control of power systems with large scale renewable energy generations,



WEI HE (Member, IEEE) received the B.Eng. and Ph.D. degrees from the School of Electrical and Electronic Engineering, Huazhong University of Science and Technology (HUST), Wuhan, China, in 2011 and 2017, respectively.

From 2017 to 2020, he was a Postdoctoral Research Associate with HUST. From 2020 to 2023, he was a Lecturer with HUST, where he has been an Associate Professor, since 2023. His current research interests include stability and control of power systems with multi-machine converters, control, and grid integration of renewable energy generations.



XIAOMING YUAN (Senior Member, IEEE) received the B.Eng. degree in electrical engineering from Shandong University, Jinan, China, in 1986, the M.Eng. degree in electrical engineering from Zhejiang University, Hangzhou, China, in 1993, and the Ph.D. degree in electrical engineering from the Federal University of Santa Catarina, Florianópolis, Brazil, in 1998.

He has been a Full Professor with the Huazhong University of Science and Technology, since 2011. He was a Chief Engineer of electrical engineering with the Global Research Center, General Electric Company, prior to his university career. He is a pioneer in the area of dynamics of power electronics dominated large power systems, and he developed the "amplitude/frequency modulation theory" for analyzing dynamics of general ac power systems.

...